J Mater Sci (2009) 44:1821–1827
DOI 10.1007/s10853-009-3248-7

# Enhanced stretch formability of Mn-free AZ31 Mg alloy rolled by cross-roll rolling

**Yasumasa Chino · Kensuke Sassa · Mamoru Mabuchi**

Received: 18 August 2008 / Accepted: 5 January 2009 / Published online: 27 January 2009


**Abstract** Stretch formability of a Mn-free AZ31 Mg alloy rolled by the reverse cross-roll rolling was investigated at room temperature. The specimen rolled by the reverse cross-roll rolling showed superior stretch formability to that of the reference specimen. The (0002) plane texture of the specimen by the revere cross-roll rolling exhibited a low texture intensity and a circular spread of the basal pole from the ND compared with those of the reference specimen. It is suggested that the modification of basal texture by the reverse cross-roll rolling contributes to an activation of basal slip and twinning, resulting in an enhancement of the thickness-direction strain and tensile ductility. Besides, it is suggested that the coarse grain size of a Mn-free AZ31 alloy seems to enhance a stretch formability, because twins become easily generated during loading.

## Introduction

Mg alloys have the high potential for improving fuel efficiency of vehicles and reducing $CO_2$ emission because of their high specific strength and stiffness [1]. For their greater applicability, it is required to advance rolling technologies for mass production of high-performance Mg alloy sheets. In Mg, the (0002) $<11\bar{2}0>$ basal slip takes place preferentially because the critical resolved shear stress (CRSS) for the basal slip is lower than those for the prismatic and pyramidal slips [2]. This gives rise to the poor ductility for a polycrystalline Mg and its alloy. Besides, for rolled Mg alloy sheets, the basal plane is strongly distributed parallel to the RD–TD plane, where the RD and TD are the rolling and transverse directions. In such a case, it is very difficult for the textured sheets to be deformed in the thickness direction [3, 4], resulting in a poor ductility under biaxial tension stress (such as under stretch-forming).

Texture control is an effective way to improve stretch formability of Mg. One of texture control ways is an addition of rare-earth (RE) metal in Mg alloy [5–7], which modifies and weakens the intensity of basal texture of rolled Mg alloys. The other approach for weakening the basal texture intensity is an imposition of shear deformation to Mg alloys such as different-speed-roll rolling [8–14]. Recently, authors [15–17] have proposed an application of the cross-roll rolling as a new method for shear deformation of Mg alloys. In the cross-roll rolling, roll axis is tilted against the TD in the RD–TD plane. Authors have revealed that a rolled Mg alloy by the cross-roll rolling exhibits an enhanced stretch formability at elevated temperature (433–493 K). The enhanced stretch formability is attributed to a low basal texture intensity [15–17].

On the other hand, recently, Ohtoshi et al. [18] have reported that rolled Mn-free AZ31 (Mg–3.0wt%Al–1.0wt%Zn) alloy exhibits an enhanced deep drawing properties at room temperature. Hence, it is suggested that an application of the cross-roll rolling to a Mn-free AZ31 alloy is effective for an improvement of stretch formability of Mg alloy at room temperature. In this article, Mn-free AZ31 alloy is rolled by the cross-roll rolling, and stretch

Y. Chino (✉) · K. Sassa
Materials Research Institute for Sustainable Development, National Institute of Advanced Industrial Science and Technology, 2266-98 Anagahora, Shimo-shidami, Moriyama-ku, Nagoya 463-8560, Japan
e-mail: y-chino@aist.go.jp

M. Mabuchi
Department of Energy Science and Technology, Graduate School of Energy Science, Kyoto University, Yoshida-honmachi, Sakyo-ku, Kyoto 606-8501, Japan

formability of the specimens is examined. Also, relationships between stretch formability, microstructure, and texture of the rolled Mn-free AZ31 alloy are discussed, because understanding of deformation behavior at room temperature for Mn-free AZ31 alloy is still insufficient.

## Experimental procedure

A specimen with 50 mm length, 60 mm width, and 3.5 mm thickness was machined from an as-received Mn-free AZ31 alloy. The specimens were heated at 618 K for $1.2 \times 10^3$ s in a furnace, and a rolling was conducted at a rolling reduction of 15%, where the roll temperature was held at 353 K. The heating and rolling treatments were repeated, and the sheet was rolled to a thickness of 1 mm. Finally, the rolled specimen was annealed at 618 K for $3.6 \times 10^3$ s. Schematic view of rolling routes is shown in Fig. 1. Two rolling routes were conducted in the present investigation. The first route was the reverse cross-roll rolling with the cross-roll angle of 7.5°, where each rolling direction changed at 180°. The second route was the unidirectional normal-roll rolling with the cross-roll angle of 0°, namely, the specimen rolled by the second route was a reference. The reason for an application of the reverse cross-roll rolling is that the reverse cross-roll rolling is more effective for weakening basal texture intensity of rolled Mg alloy sheet than the unidirectional cross-roll rolling [17]. Here after, the specimen rolled by the first and second routes is called the specimen A and specimen B, respectively.

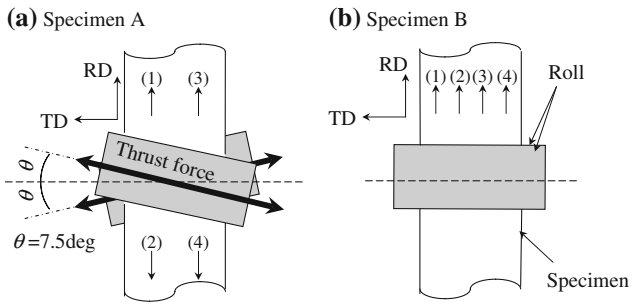


**Fig. 1** Schematic view of rolling routes: **a** reverse cross-roll rolling and **b** unidirectional normal-roll rolling, hereafter the specimen rolled by the reverse cross-roll rolling and the unidirectional normal-roll rolling is called specimen A and specimen B, respectively

A circular blank with a diameter of 60 mm was machined from the specimens. Erichsen tests [19] using a hemispherical punch with a diameter of 20 mm were carried out at room temperature to investigate the stretch formability of the specimens, and the Erichsen value (IE), which was the punch stroke at fracture initiation, was measured. Tensile specimens with 10 mm gage length, 5 mm gage width, and 1 mm gage thickness were machined from the specimens. Tensile tests were carried out at room temperature with an initial strain rate of $1.7 \times 10^{-3}$ $s^{-1}$, where the angles between tensile direction and RD were 0, 45, and 90°. Additional tensile tests were conducted to investigate the Lankford value ($r$-value, $r = \varepsilon_w/\varepsilon_t$). The width direction strain ($\varepsilon_w$) and the thickness direction strain ($\varepsilon_t$) were measured using the specimens deformed to 10% nominal strain.

A microstructure of rolled Mg alloys was investigated by optical microscopy. Grain size of the specimens was determined by intercept method [20]. Also, twin area ratio of the specimen tensile deformed to 10% nominal strain was estimated by quantitative image analysis using the commercially available software Image-Pro Plus for calculating the area of all present twins and relating this area to the total area of the micrograph. A (0002) plane pole figure of rolled Mg alloy sheets at center through a thickness was investigated by Schulz reflection method. The data were normalized by powder Mg data. A Schmid factor map of rolled Mg alloys was investigated by electron back scattering pattern (EBSP) mapping analysis.

## Results

A microstructure of the specimens A and B of the TD–ND plane is shown in Fig. 2, where ND is the normal direction.

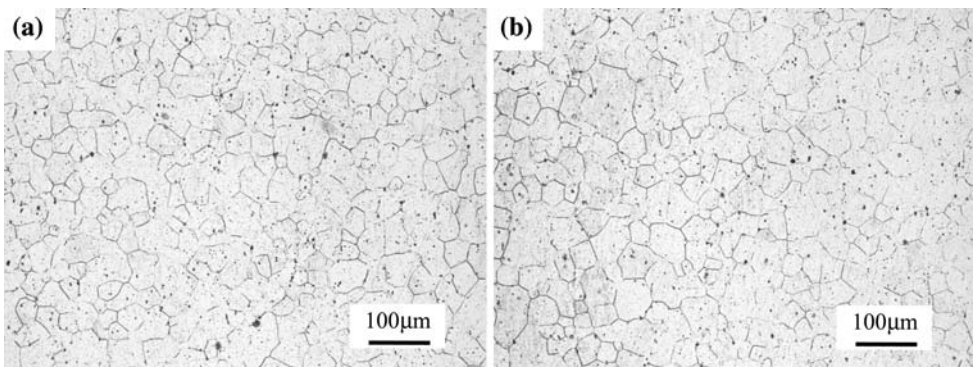


**Fig. 2** Optical micrograph of the rolled Mn-free AZ31 alloys after annealing, where the TD–ND plane is observed: **a** specimen A and **b** specimen B

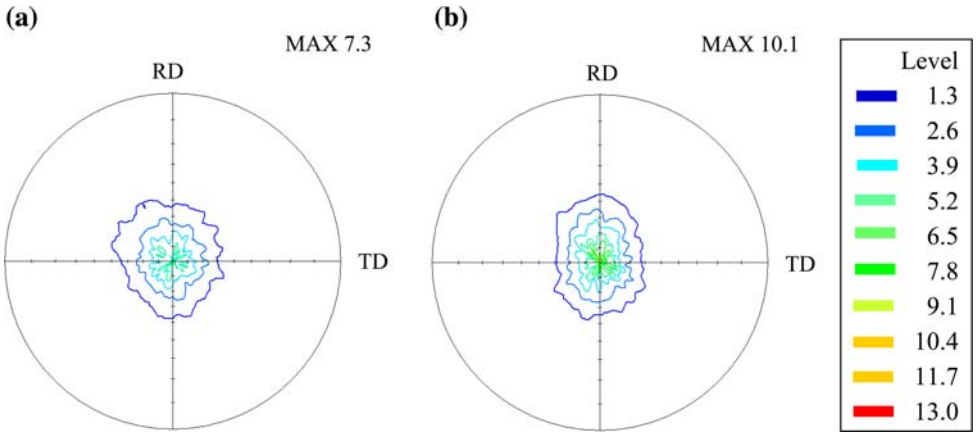


**Fig. 3** The (0002) pole figure of the rolled Mn-free AZ31 alloys, where the pole figure was measured at center through a thickness of the specimens: **a** specimen A and **b** specimen B

The average grain size obtained from observations of the RD–TD, RD–ND, and TD–ND planes was 40 and 44 μm for the specimens A and B, respectively. There was a little difference in grain size between them. The smaller grain size of the specimen A than the specimen B is attributed to an intense shear straining by the cross-roll rolling [16].

The (0002) plane pole figure of the specimens A and B is summarized in Fig. 3. The (0002) plane of the specimen B was intensively distributed parallel to the RD–TD plane, and there was a spreading of the basal pole toward the RD. The similar tendency was observed in the specimen A, although there were minor differences, namely, there was a circular spread of the basal pole from the ND. Besides, the basal texture of the specimen A showed much lower intensity than that of the specimen B, indicating that shear deformation by the reverse cross-roll rolling effectively modified and weakened the basal texture in the same manner with the previous study [17].

Figure 4 shows the Schmid factor mapping by EBSP for the basal <a> slip of the specimens A and B, when the tensile stress is applied in the RD, and where the RD–TD plane at center through a thickness is observed. The Schmid factor for the basal <a> slip is defined as $S_{\text{basal}} = \cos\chi\cos\lambda$, where $\chi$ is the angle between the ND of a basal plane and the stress axis, and $\lambda$ is the angle between the $<11\bar{2}0>$ direction and the stress axis. The fraction of grains with high-Schmid factor ($S_{\text{basal}} = 0.4$–$0.5$) was 0.28 for specimen A and 0.22 for the specimen B, showing that the specimen A had more grains preferable for the basal <a> slip during tensile deformation. This is directly related to the weaker basal texture intensity for the specimen rolled by the reverse cross-roll rolling.

The results of Erichsen tests at room temperature are summarized in Fig. 5. The specimen A exhibited 1.3 times larger Erichsen value (IE = 6.0) than the specimen B (IE = 4.7). It is recognized that the basal texture intensity significantly affects the stretch formability of Mg alloys [8, 14–17]. Clearly, the superior stretch formability of the specimen A results from the weak intensity of basal texture.

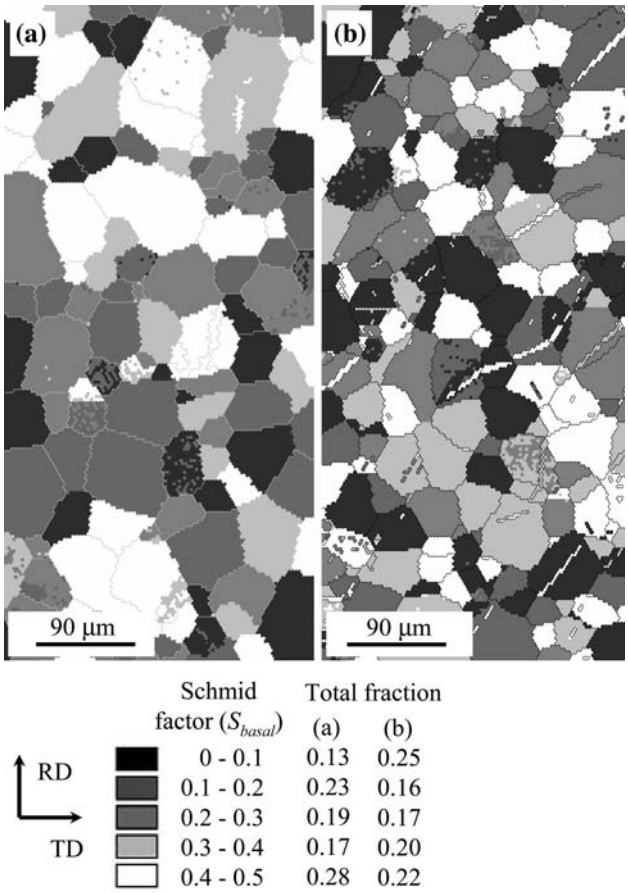


**Fig. 4** Schmid factor mapping by EBSP analysis for the rolled Mn-free AZ31 alloys: **a** specimen A and **b** specimen B

The $r$-values and their average $r$-value ($\bar{r} = |(r_0 + 2r_{45} + r_{90})/4|$) are shown in Fig. 6, where $r_0$, $r_{45}$, and $r_{90}$ are the $r$-values at the angles between tensile direction and RD of 0, 45 and 90°, respectively. Note that the average $r$-value of the specimen A ($\bar{r} = 1.6$) was much lower than that of the specimen B ($\bar{r} = 3.1$). This is because the thickness-direction strain occurred more for the specimen A. Indeed, the thickness-direction strain at the top part of

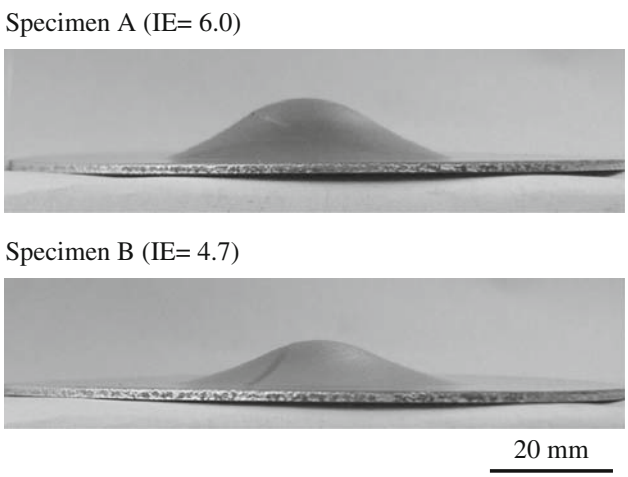


**Fig. 5** Specimens after the Erichsen test at room temperature for the rolled Mn-free AZ31 alloys

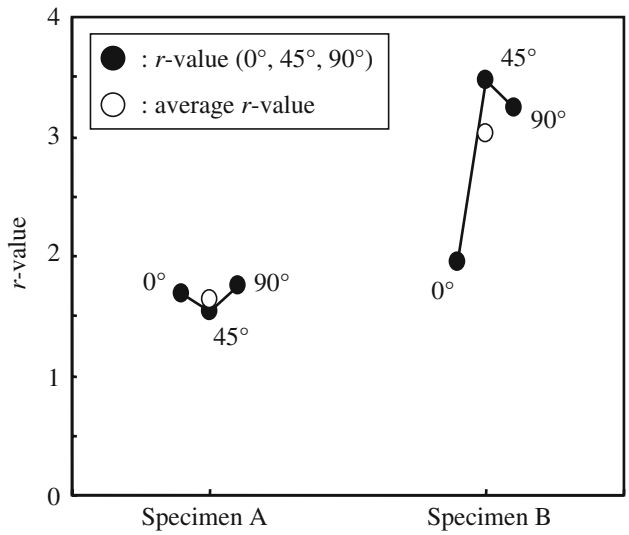


**Fig. 6** *r*-values of the rolled Mn-free AZ31 alloys and their average *r*-value

the specimens A and B after the Erichsen test was 0.16 and 0.08, respectively, which was estimated by measuring the thickness of specimens before and after the Erichsen tests. Under biaxial tensile stress, the negative thickness-direction strain must be obtained since both the positive tensile-direction and width-direction strains occur. However, it is difficult for the basal textured Mg alloy to be sufficiently deformed in the thickness direction [3, 4]. This means that a weak basal texture intensity, in other words, a high fraction of grains with high-Schmid factor for basal slip, is essential for an enhancement of stretch formability of a Mg alloy sheet. Hence, it is evident that the weak basal texture intensity of the specimen A contributes to the high thickness-direction strain, resulting in the enhanced stretch formability. It should be noted that the *r*-values at 45 and 90° of the specimen A were much lower than those of the specimen B. It seems that the reduction of anisotropy for *r*-values also contributes to the enhancement of macroscopic thickness-direction strain. It is likely that the low anisotropy of *r*-values of the specimen A is originated from not only the weak basal texture intensity but also the circular spread of the basal pole from the ND.

The 0.2% proof stress and elongation to failure obtained by tensile tests are shown in Fig. 7. At all the angles, the specimen A exhibited higher tensile elongation of around 25% compared with the specimen B (around 20%) regardless of the little difference in grain size. It is suggested that the weak basal texture intensity contributes to not only an improvement of thickness-direction strain but also tensile ductility.

Thus, it is demonstrated that the reverse cross-roll rolling is effective for improving the stretch formability of rolled Mg alloys not only at elevated temperature [17] but also at room temperature. The superior stretch formability of the specimen by the reverse cross-roll rolling is attributed to the enhancement of not only thickness-direction

**Fig. 7** The variation in 0.2% proof stress and elongation to failure as a function of the angle between tensile direction and RD for the rolled Mn-free AZ31 alloys

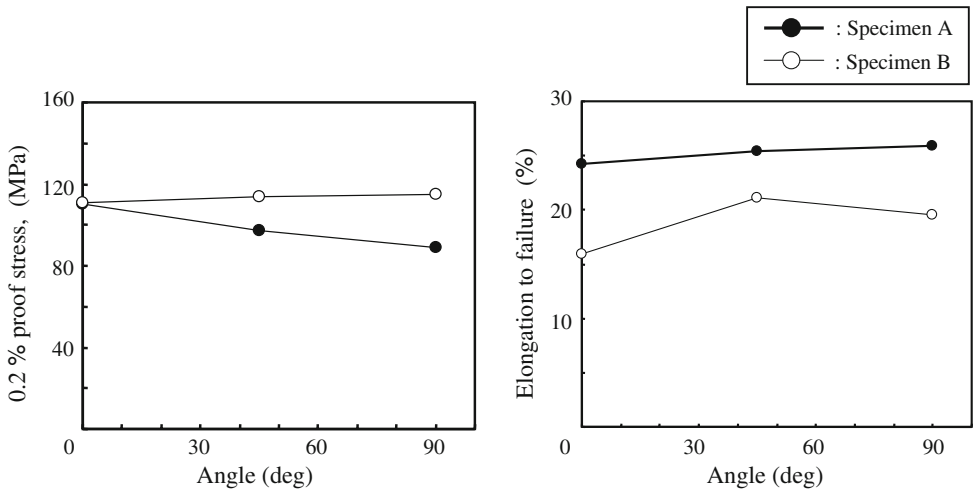

strain but also tensile ductility resulting from the basal texture modification.

## Discussion

The tensile elongation and stretch formability balance in the AZ31B (Mg–3.0wt%Al–1.0wt%Zn–0.5wt%Mn) alloys [4, 14, 21, 22] and the rolled Mn-free AZ31 alloys are shown in Fig. 8. Also, the data for 5083 Al alloy are included [23]. The Mn-free AZ31 alloy rolled by the reverse cross-roll rolling (specimen A) showed the good balance with tensile elongation and stretch formability compared with the rolled AZ31B alloys. It is noted that the stretch formability of the specimen A took the 72% value of that of 5083 Al alloy. On the other hand, partially noteworthy is that the specimen B exhibited the same or higher stretch formability compared with the AZ31B alloys despite the minor tensile elongation. This indicates that an application of Mn-free AZ31 alloy makes a contribution to high ductility under biaxial tensile stress (stretch formability) rather than high ductility under uniaxial tensile stress (tensile ductility). In this section, the effects of Mn addition on the stretch formability of AZ31 alloy are briefly discussed.

Table 1 lists elongation to failure, Erichsen value, grain size and basal texture intensity of rolled AZ31B alloys [14, 15, 17, 22] and rolled Mn-free AZ31 alloys. Note that the grain size of Mn-free AZ31 alloys (around 40 μm) was much coarser than that of the AZ31B alloys (around 10 μm). This is because second particles (such as $Al_8Mn_5$) [24] in the AZ31B alloys effectively pin a grain growth during hot rolling. Koike et al. [3] reported that under uniaxial tensile stress, a negative width-direction strain associated with an activation of the prismatic <a> slip balances with a positive tensile-direction strain in the case of Mg alloys with small grain size (around 10 μm). Thus, the ambient tensile elongation of the rolled AZ31B alloys in Fig. 8 results from a localized necking of the tensile specimen in the width direction.

In general, coarse second hard particles in metallic materials become the sites for stress concentration and void nucleation [25]. It is known that Mn addition more than 0.15 wt% in AZ31 alloy promotes precipitation of a large amount of coarse Al–Mn particles [26, 27]. One possible origin for the high stretch formability of Mn-free AZ31 alloys is a variation of fracture mechanisms by the presence or not of coarse Al–Mn particles. However, previous studies [24, 26, 27] have reported that there is no difference in tensile elongation between Mn-free AZ31 alloy and AZ31 alloy with Mn addition of more than 0.25 wt%. This indicates that a void nucleation around Al–Mn particles does not necessarily play an important role in the fracture mechanism of AZ31B alloy.

As described in the section "Results," a high thickness-direction strain is essential for an enhancement of stretch formability. Another possible origin for the high stretch formability of Mn-free AZ31 alloys is a difference in basal texture intensity. However, as shown in Table 1, the magnitude of basal texture intensity for Mn-free AZ31 alloys was almost the same as that for AZ31B alloys. Therefore, it is likely that the superior stretch formability of Mn-free AZ31 alloys cannot be explained by the basal texture intensity.

Most likely origin for the superior stretch formability of Mn-free AZ31 alloys is a variation of twinning behaviors originated from a difference in grain size. Figure 9 shows microstructures of the specimens A and B deformed to 10% nominal strain by tensile tests, where the TD–ND plane is observed. More deformation twins were observed in the specimen A. The twin area ratio measured by the image analysis was 10.0% for the specimen A and 5.5% for the specimen B. It is reported that $\{10\bar{1}2\}$ twins become easily generated during tensile loading due to the high

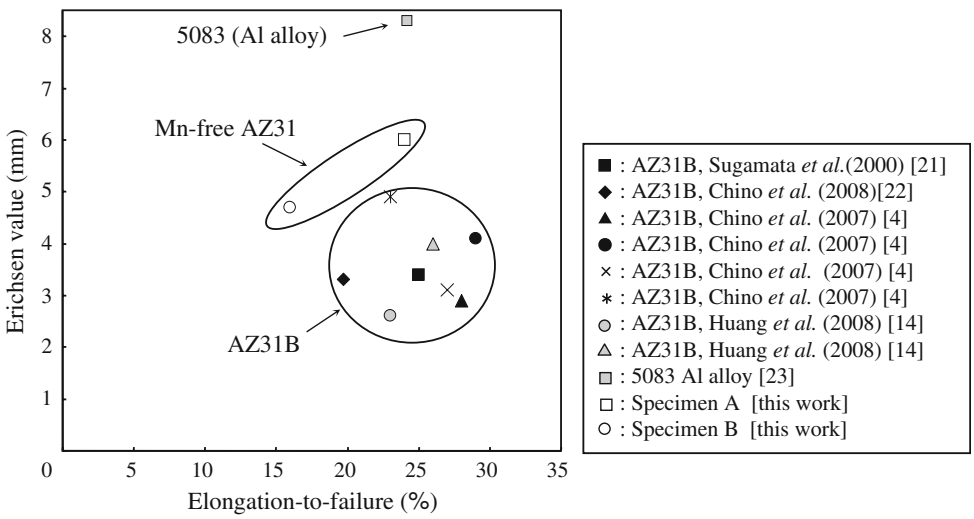


**Fig. 8** Relationships between tensile elongation (elongation-to-failure) and stretch formability (Erichsen value) in the rolled AZ31B alloys and the rolled Mn-free AZ31 alloys, where the tensile elongation, whose tensile direction was parallel to RD, is adopted. Included is the data for 5083 Al alloy [4, 14, 21–23]

**Table 1** Elongation-to-failure, Erichsen value, and microstructural properties of rolled AZ31B alloys and rolled Mn-free AZ31 alloys, where the tensile elongation, whose tensile direction was parallel to the RD, is adopted, and the basal texture intensity, where the pole figure was measured at center through a thickness and normalized by powder Mg data, is adopted [14, 15, 17, 22]

| | Materials | Rolling temperature (K) | Rolling method | Elongation to failure (%) | Erichsen value (mm) | Grain size (μm) | Basal texture intensity (−) | Reference |
|---|---|---|---|---|---|---|---|---|
| 1 | AZ31B | 603 | Normal-roll rolling (unidirectional) | 78 (at 433 K) | 3.5 (at 433 K) | 10 | 8.2 | [15] |
| 2 | AZ31B | 673 | Cross-roll rolling (unidirectional) | 72 (at 433 K) | 6.4 (at 433 K) | 11 | 6.2 | [17] |
| 3 | AZ31B | 673 | Cross-roll rolling (reverse) | 76 (at 433 K) | 6.8 (at 433 K) | 10 | 5.9 | [17] |
| 4 | AZ31B | 703 and 573 | Normal-roll rolling (reverse) | 23 (at RT) | 2.6 (at RT) | 16 | 10.6 | [14] |
| 5 | AZ31B | 703 and 573 | Different-speed-roll rolling (reverse) | 26.0 (at RT) | 4.0 (at RT) | 16 | 8.8 | [14] |
| 6 | AZ31B | 663 | Normal-roll rolling (unidirectional) | 25.0 (at RT) | 3.4 (at RT) | 11 | 10.2 | [22] |
| 7 | AZ31 | 618 | Cross-roll rolling (reverse) | 24.0 (at RT) | 6.0 (at RT) | 40 | 7.3 | This work |
| 8 | AZ31 | 618 | Normal-roll rolling (unidirectional) | 16.0 (at RT) | 4.7 (at RT) | 44 | 10.1 | This work |

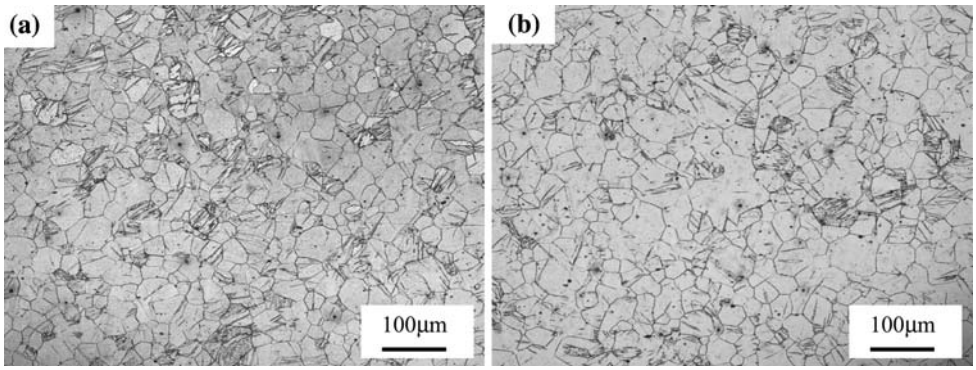


**Fig. 9** Optical micrograph of the rolled Mn-free AZ31 alloys tensile deformed to 10% nominal strain, where the angle of tensile direction and RD is 90°, and the TD–ND plane is observed: **a** specimen A and **b** specimen B

Schmid factor for twinning, when Mg alloys exhibit a weak basal texture intensity [28, 29]. This may be responsible for the larger twin area ratio of the specimen A than the specimen B. On the other hand, it is worthy of special mention that the twin area ratio of the specimen B is still much larger than that of the AZ31B alloy [29]. In our previous study [29], the much small twin area ratio of 1.0% was observed in the AZ31B extrusions tensile-deformed to 16% nominal strain, whose grain size was 8 μm. It is known that energy of twin interfaces is significantly large in Mg and twin nucleation decreases with decreasing grain size [30], that is, twin formation is enhanced by grain coarsening. Therefore, it is suggested that large grain size of Mn-free AZ31 alloys significantly promotes twin generation during tensile deformation. Our previous study [31] has revealed that stretch formability of rolled AZ31B alloy is improved with an increase in grain size. The enhanced stretch formability of the AZ31B alloy with coarse grain size is suggested to be closely related to a generation of $\{10\bar{1}1\}$ twins. When $\{10\bar{1}1\}$ twins are formed, the basal plane in the twin is inclined at 56° to the basal plane in the matrix grain [32]. Such a lattice rotation results in an increase in Schmid factor for the basal slip in the twin, and thereby the basal slip in the twin is activated. Therefore, it is suggested that the enhanced basal slip due to lattice rotation by $\{10\bar{1}1\}$ twinning plays a critical role inducing high thickness-direction strain of Mn-free AZ31 alloys.

## Conclusions

Stretch formability of the Mn-free AZ31 Mg alloys rolled by the reverse cross-roll rolling was investigated at room temperature, and origins of the enhanced stretch formability of rolled Mn-free AZ31 alloys by the reverse cross-roll rolling were discussed.

A Mn-free AZ31 alloy rolled by the reverse cross-roll rolling showed superior stretch formability and tensile elongation to that of the reference Mn-free AZ31 alloy. The (0002) plane texture of the specimen by the revere

cross-roll rolling exhibited a low texture intensity and a circular spread of the basal pole from ND compared with those of the reference specimen. It is suggested that the modification of basal texture by the reverse cross-roll rolling contributes to an activation of basal slip and twinning, resulting in an enhancement of the thickness-direction strain and tensile ductility. Besides, it is suggested that coarse grain size of a Mn-free AZ31 alloy seems to enhance a stretch formability, because twins become easily generated during loading.

## References


1. Hakamada M, Furuta T, Chino Y, Chen Y, Kusuda H, Mabuchi M (2007) Energy 32:1352
2. Yoshinaga H, Horiuchi R (1963) Trans JIM 4:1
3. Koike J, Ohyama R (2005) Acta Mater 53:1963
4. Chino Y, Iwasaki H, Mabuchi M (2007) Mater Sci Eng A 466:90
5. Bohlen J, Nürnberg MR, Senn JW, Letzig D, Agnew SR (2007) Acta Mater 55:2101
6. Stanford N, Barnett M (2008) Scripta Mater 58:179
7. Chino Y, Kado M, Mabuchi M (2008) Mater Sci Eng A 494:343
8. Chino Y, Mabuchi M, Kishihara R, Hosokawa H, Yamada Y, Wen CE, Shimojima K, Iwasaki H (2002) Mater Trans 43:2554
9. Watanabe H, Mukai T, Ishikawa K (2004) J Mater Sci Lett 39:1477
10. Kim SH, You BS, Yim CD, Seo YM (2005) Mater Lett 59:3876
11. Watanabe H, Mukai T, Ishikawa K (2007) J Mater Process Technol 182:644
12. Huang X, Suzuki K, Watazu A, Shigematsu I, Saito N (2008) J Alloys Compd 475:408
13. Huang X, Suzuki K, Watazu A, Shigematsu I, Saito N (2008) Mater Sci Eng A 488:214
14. Huang X, Suzuki K, Watazu A, Shigematsu I, Saito N (2008) J Alloys Compd. doi:10.1016/j.jallcom.2008.02.029
15. Chino Y, Sassa K, Kamiya A, Mabuchi M (2006) Mater Sci Eng A 441:349
16. Chino Y, Sassa K, Kamiya A, Mabuchi M (2007) Mater Lett 61:1504
17. Chino Y, Sassa K, Kamiya A, Mabuchi M (2008) Mater Sci Eng A 473:195
18. Ohtoshi K, Nagayama T, Katsuta M (2003) J Jpn Inst Light Met 53:239
19. In ISO 20482 (2003) Metallic materials—sheet and strip—Erichsen cupping test
20. Thompson AW (1972) Metallography 28:366
21. Sugamata M, Kaneko J, Numa M (2000) J Jpn Soc Technol Plast 41:233
22. Chino Y, Mabuchi M (2009) Scripta Mater 60:447
23. Japan Light Metal Association (2000) Aluminum handbook, 4th edn. Japan Light Metal Association, Tokyo
24. Laser T, Nürnberg M, Janz A, Hartig Ch, Letzig D, Schmid-Fetzer R, Bormann R (2006) Acta Mater 54:3033
25. Tanaka K, Mori T, Nakamura T (1970) Philos Mag 21:267
26. Yoshida Y, Cisar L, Sekine T, Kamado S, Kojima Y (2004) J Jpn Inst Met 68:412
27. Sasaki T, Takigawa Y, Higashi K (2008) Mater Sci Eng A 479:117
28. Kleiner S, Uggowitzer PJ (2004) Mater Sci Eng A 379:258
29. Chino Y, Kimura K, Mabuchi M (2008) Mater Sci Eng A 486:481
30. Koike J, Kobayashi T, Mukai T, Watanabe H, Suzuki M, Maruyama K, Higashi K (2003) Acta Mater 52:2055
31. Chino Y, Kimura K, Mabuchi M (2008) Acta Mater. doi:10.1016/j.actamat.2008.11.033
32. Nave MD, Barnett MR (2004) Scripta Mater 51:881